

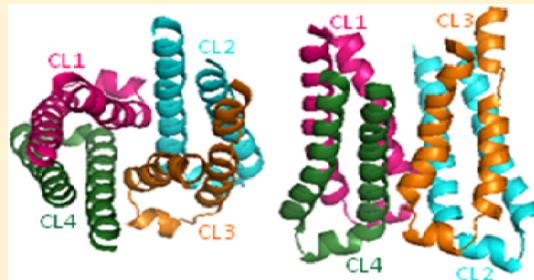
# Role of the Juxtamembrane Region of Cytoplasmic Loop 3 in the Gating and Conductance of the Cystic Fibrosis Transmembrane Conductance Regulator Chloride Channel

Yassine El Hiani and Paul Linsdell\*

Department of Physiology and Biophysics, Dalhousie University, Halifax, Nova Scotia B3H 4R2, Canada

 Supporting Information

**ABSTRACT:** Opening and closing of the cystic fibrosis transmembrane conductance regulator chloride channel are controlled by interactions of ATP with its cytoplasmic nucleotide binding domains (NBDs). The NBDs are connected to the transmembrane pore via four cytoplasmic loops. These loops have been suggested to play roles both in channel gating and in forming a cytoplasmic extension of the channel pore. To investigate the structure and function of one of these cytoplasmic loops, we have used patch clamp recording to investigate the accessibility of cytoplasmically applied cysteine-reactive reagents to cysteines introduced into loop 3. We find that methanethiosulfonate (MTS) reagents modify cysteines introduced at 14 of 16 sites studied in the juxtamembrane region of loop 3, in all cases leading to inhibition of channel function. In most cases, both the functional effects of modification and the rate of modification were similar for negatively and positively charged MTS reagents. Single-channel recordings indicated that, at all sites, inhibition was the result of an MTS reagent-induced decrease in channel open probability; in no case was the Cl<sup>-</sup> conductance of open channels altered by modification. These results indicate that loop 3 is readily accessible to the cytoplasm and support the involvement of this region in the control of channel gating. However, our results do not support the hypothesis that this region is close enough to the Cl<sup>-</sup> permeation pathway to exert any influence on permeating Cl<sup>-</sup> ions. We propose that either the cytoplasmic pore is very wide or cytoplasmic Cl<sup>-</sup> ions use other routes to access the transmembrane pore.



Cystic fibrosis is caused by loss of function mutations in the cystic fibrosis transmembrane conductance regulator (CFTR) Cl<sup>-</sup> channel, a member of the ATP-binding cassette (ABC) family of ATP-dependent membrane transport proteins. All ABC proteins share a common modular architecture, consisting of two membrane-spanning domains (MSDs) that form the substrate translocation pathway and two cytoplasmic nucleotide binding domains (NBDs) that bind and hydrolyze ATP (Figure 1). In CFTR, an additional cytoplasmic regulatory domain (R domain) is the site of regulation by PKA-dependent phosphorylation. Consistent with this ABC architecture, several transmembrane (TM)  $\alpha$ -helices<sup>1–3</sup> and extracellular loops (ELs)<sup>4,5</sup> have been shown to contribute to the Cl<sup>-</sup> channel pore in CFTR. The activity of the channel is controlled by ATP interactions at the NBDs,<sup>6,7</sup> which leads to the opening and closing of a “gate” located in the MSDs.<sup>8</sup>

The NBDs are not in direct contact with the TMs but instead are connected indirectly via the long cytoplasmic loops (CLs) that are located between individual TMs (Figure 1). Structural models of the CFTR protein<sup>9–11</sup> therefore suggest that NBD–CL interactions should be important in coupling ATP action at the NBDs to channel opening in the MSDs. In fact, the role of the CLs in forming a physical and functional link between the NBDs and the transmembrane substrate translocation pathway may be conserved among all ABC proteins.<sup>12,13</sup> The location of the CLs below the TMs (Figure 1A) also suggests that the CLs

could form a cytoplasmic extension of the permeation pathway for Cl<sup>-</sup> ions. In fact, on the basis of these models, it has been suggested that the CLs form a narrow “funnel” connecting the TMs to the cytoplasm (Figure 1C), and that this CL funnel, not the TMs, forms the narrowest part of the Cl<sup>-</sup> channel pore where channel opening and closing may occur.<sup>11</sup>

Functional evidence also supports a role for NBD–CL interactions in ATP-dependent channel gating (pore opening and closing). For example, CL3, located between TM8 and TM9 (Figure 1), interacts with both NBDs<sup>14</sup> as well as the R domain<sup>15,16</sup> to regulate gating. Mutations within CL3 also affect gating,<sup>17,18</sup> perhaps by disrupting communication between the NBDs and the gate in the MSDs.<sup>19</sup> CF-associated mutations in this loop also disrupt processing and trafficking of CFTR protein to the membrane,<sup>17,20</sup> perhaps highlighting the importance of domain–domain interactions in proper protein folding,<sup>10,21–23</sup> although CL3 has also been implicated in ubiquitination-dependent CFTR trafficking.<sup>24</sup> There is also some functional evidence that CL3 may contribute to the Cl<sup>-</sup> permeation pathway. The CF-associated mutations S945L and G970R were shown to have very slightly altered single-channel Cl<sup>-</sup> conductance.<sup>17</sup> Furthermore, the positive charge associated

Received: January 16, 2012

Revised: April 30, 2012

Published: April 30, 2012

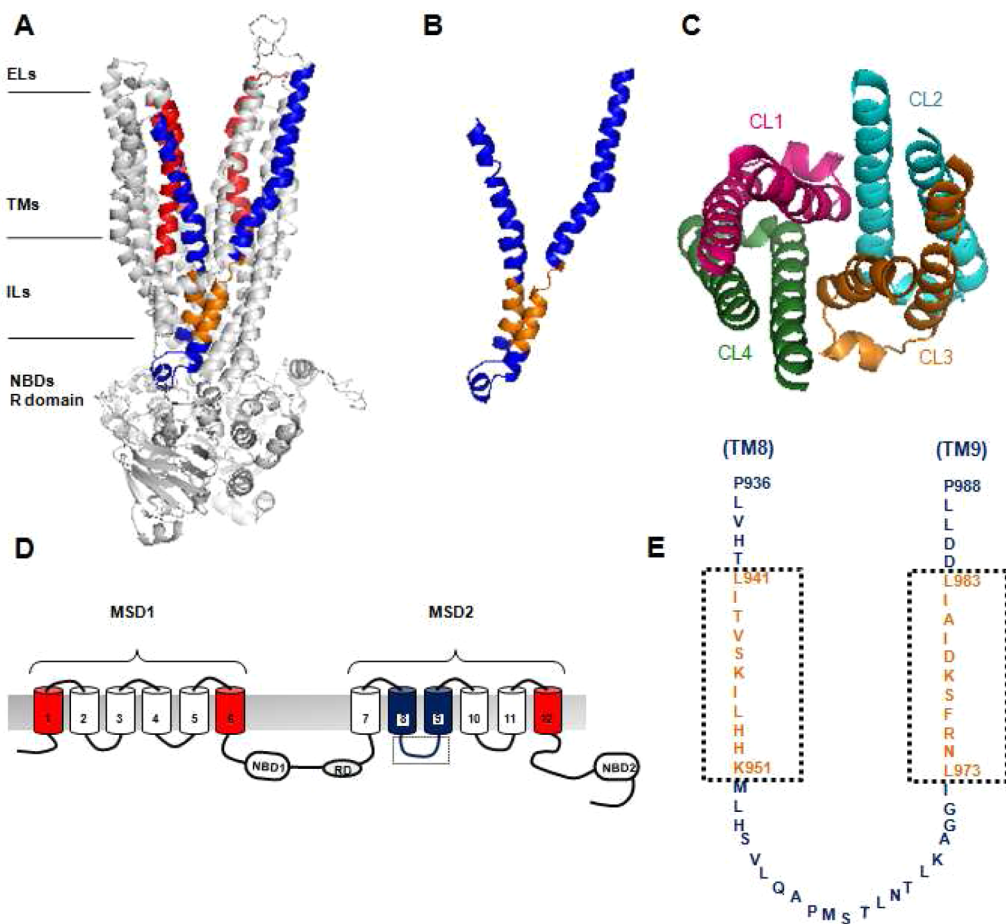


**Figure 1.** Location of CL3 within the overall structure of CFTR. The CFTR protein consists of two MSDs and two NBDs, joined by a cytoplasmic R domain. Each MSD consists of six TM helices connected by three ELs and two CLs. (A) Proposed overall structure of CFTR (viewed from the side), based on atomic homology modeling of bacterial ABC protein Sav1866.<sup>10</sup> TMs that are known to line the Cl<sup>-</sup> channel pore are colored red (from left to right, TM1, TM6, and TM12, respectively). The locations of TM8 (left) and TM9 (right) are colored blue. Connecting these two TMs is CL3, which is colored blue, with the region mutated in this study colored gold. (B) Isolated TM8-CL3-TM9 region from the same model, showing the juxtamembrane region of this CL as a cytoplasmic extension of these two TMs. (C) Position of the CLs around a narrow “funnel” region in the cytoplasm, as viewed from above. Other parts of the protein have been removed for the sake of clarity. The part of CL3 that appears to line this narrow region is that proximal to TM9. Illustrations were prepared using PyMOL based on the structure presented by Serohijos et al.<sup>10</sup> (D) Two-dimensional topology of CFTR, illustrating two MSDs, two NBDs, the R domain (RD), and 12 TMs. The coloring of the TMs is the same as that in panel A. The region mutated in this study is enclosed in the dotted box, which is magnified in panel E. This shows the amino acid sequence of CL3, from P936 at the cytoplasmic end of TM8 to P988 at the cytoplasmic end of TM9. As in panels A–C, residues mutated in this study (L941–K951 and L973–L983) are colored gold.

with CL3 residue K978 is involved in interactions with cytoplasmic channel blocking substances.<sup>25,26</sup> However, the role of CL3 in channel function has not previously been addressed in a comprehensive way.

To investigate the possibility that CL3 forms a cytoplasmic extension of the CFTR pore, we have undertaken a substituted cysteine accessibility mutagenesis (SCAM) study of the juxtamembrane parts of this loop. Because residues within the CLs have not previously been directly demonstrated to contribute to the permeation pathway, we reasoned that this region relatively close to the TMs might be considered most likely to influence Cl<sup>-</sup> permeation. Furthermore, more cytoplasmic parts of CL3 are likely to be involved in interactions with NBD1.<sup>9,10,14</sup> We have used SCAM because of the proven power of this approach in identifying amino acids that contribute to the CFTR permeation pathway.<sup>2,3,27–30</sup> Our results indicate that the juxtamembrane regions of CL3 are exposed to the cytoplasm and are readily modified by

intracellular cysteine-reactive methanethiosulfonate (MTS) reagents. However, the effects of modification appear to reflect changes in channel gating, rather than channel permeation properties. These results suggest that while CL3 plays a role in the coordination of ATP-dependent gating, it does not make an important functional contribution to the Cl<sup>-</sup> permeation pathway.

## MATERIALS AND METHODS

Experiments were conducted on baby hamster kidney (BHK) cells transiently transfected with CFTR. As in our recent SCAM-based studies of individual TMs,<sup>2,28,30</sup> we have used a human CFTR variant from which all cysteines had been removed by mutagenesis (as described in ref 31) and which includes a mutation in NBD1 (V510A) to increase the level of protein expression in the cell membrane.<sup>32</sup> Use of this Cys-less variant is necessary for these studies because wild-type CFTR is potently inhibited by cytoplasmic MTS reagents.<sup>33</sup> However, in

addition to its severe trafficking defect,<sup>34,35</sup> Cys-less CFTR has been reported to have gating<sup>31,36</sup> and permeation<sup>31,36,37</sup> properties subtly different from those of wild-type CFTR. Additional mutations were introduced into the Cys-less background using the QuikChange site-directed mutagenesis system (Agilent Technologies, Santa Clara, CA) and verified by DNA sequencing. Mutations were introduced into the juxtamembrane regions of CL3, replacing each consecutive amino acid between L941 and K951 (in the cytoplasmic extension from TM8) and from L973 to L983 (in the cytoplasmic extension from TM9) individually with cysteine (Figure 1E). BHK cells were transiently transfected as described previously,<sup>38</sup> except that 24 h after transfection cells were transferred to 27 °C to promote mature protein expression.<sup>32</sup> Cells were used for Western blotting analysis after 48 h at 27 °C, and for electrophysiological experimentation after 1–3 days at 27 °C.

For Western blotting, cells at ~80% confluence were washed twice with ice-cold PBS, harvested by being scraped, and lysed on ice for 30 min in RIPA buffer supplemented with protease inhibitors. Cells were lysed by repeated vortexing as well as by passing the lysate through a pipet tip every 5 min. The lysate was then centrifuged (15000g for 30 min at 4 °C) and the supernatant poured into a fresh tube. The protein concentration was assayed using the Bradford protein assay method. Approximately 30 µg of protein was preincubated with an equal volume of loading buffer for 30 min at 37 °C and then loaded onto a 7.5% acrylamide–SDS gel and finally transferred to an Immobilon-P membrane (Millipore, Bedford, MA). Immunoblotting for CFTR was performed by incubating the membrane overnight at 4 °C with monoclonal mouse anti-CFTR antibody (M3A7, Millipore) at a 1:1000 dilution. After being washed, the membrane was incubated for 1 h at room temperature with a secondary antibody (horseradish peroxidase-conjugated goat anti-mouse, Jackson ImmunoResearch, West Grove, PA) at a 1:5000 dilution. Detection was conducted using the ECL Plus kit (Amersham Pharmacia, Baie d'Urfe, QC) following the manufacturer's instructions. The relative expression of mature, complex glycosylated CFTR protein ("Band C") and immature, core glycosylated protein ("Band B") was assessed by densitometric analysis of scanned Western blots using 1-D (Bio-Rad, Hercules, CA).

Macroscopic and single-channel recordings were made using the excised, inside-out configuration of the patch clamp technique. CFTR channels were activated after patch excision and recording of background currents by exposure to protein kinase A catalytic subunit (PKA, 20 nM) and MgATP (1 mM) in the cytoplasmic solution. For macroscopic current recordings, both the intracellular (bath) and extracellular (pipet) solution contained 150 mM NaCl, 10 mM N-tris(hydroxymethyl)methyl-2-aminoethanesulfonate, and 2 mM MgCl<sub>2</sub>. For single-channel recordings, NaCl in the pipet solution was replaced with 150 mM sodium gluconate to generate an outwardly directed Cl<sup>-</sup> concentration gradient. This was done to allow CFTR single-channel currents to be resolved at a membrane potential of -20 mV during the prolonged recordings necessary for measurement of channel open probability (see Figure 7). During preliminary recordings, we found that inside-out patches held at more negative or positive membrane potentials using the same symmetrical Cl<sup>-</sup> solutions used for macroscopic current recordings were unstable over these prolonged recording periods. The transmembrane Cl<sup>-</sup> concentration gradient is not expected to

influence any of the parameters measured in our experiments. All experimental solutions were adjusted to pH 7.4.

Channels were exposed to intracellular cysteine-reactive MTS reagents to covalently modify an introduced cysteine side chain. Two MTS reagents, the negatively charged [2-sulfonatoethyl] MTS (MTSES) and the positively charged [2-(trimethylammonium)ethyl] MTS (MTSET) were used at high concentrations (200 µM) that had no effect on Cys-less CFTR.<sup>28,32</sup> MTS reagents were applied to the cytoplasmic face of inside-out patches after stable current activation with PKA and ATP, and the current was monitored for at least 5 min to ensure stable modification. In some cases, the identity of the remaining currents as being carried by CFTR was confirmed using the CFTR-specific inhibitor CFTR<sub>inh</sub>-172. To measure the rate of modification, the macroscopic current amplitude was monitored continuously and the time-dependent change in amplitude after the addition of MTS reagent was fitted by a single-exponential function. The time constant of exponential current decay,  $\tau$ , was then used to calculate the apparent second-order reaction rate constant,  $k$ , from the equation  $k = 1/([MTS]\tau)$ .

Current traces were filtered at 100 Hz (macroscopic currents) or 50 Hz (single-channel currents) using an eight-pole Bessel filter, digitized at 250 Hz, and analyzed using pCLAMP9 (Molecular Devices, Sunnyvale, CA). Macroscopic current–voltage ( $I$ – $V$ ) relationships were constructed using voltage ramp protocols from a holding potential of 0 mV. The single-channel current amplitude and channel open probability were estimated from all-points amplitude histograms (Figure 7). For analysis of the effects of MTSES on single-channel currents, currents were recorded for at least 5 min at a membrane potential of -20 mV under control conditions to ensure stable channel activity, following which MTSES was applied to the cytoplasmic face of the patch and currents were recorded for a further 5–12 min. Because channel open probability was highly variable between patches (see Figure S2 of the Supporting Information), we have focused on the effect of MTSES exposure on open probability, which we found to be considerably more consistent (Figure 8B).

Experiments were conducted at room temperature (21–24 °C). Values are presented as means  $\pm$  the standard error of the mean. Tests of significance were conducted using an unpaired  $t$  test, for which  $p < 0.05$  was considered statistically significant. All chemicals were obtained from Sigma-Aldrich (Oakville, ON), except MTSES and MTSET (Toronto Research Chemicals, North York, ON) and PKA (Promega, Madison, WI).

## RESULTS

**Expression of CL3 Mutants in a Cys-less CFTR Background.** We used site-directed mutagenesis to introduce cysteines into the juxtamembrane region of CL3 (Figure 1). Cysteines were substituted for each amino acid from L941 to K951 in the cytoplasmic extension from TM8, and from L973 to L983 in the extension from TM9 (Figure 1E). Mutant CFTR was expressed in BHK cells, and proper processing of the CFTR protein was assayed using Western blot analysis. As shown in Figure 2, Cys-less CFTR was able to generate mature, complex glycosylated (Band C) protein, although the relative abundance of this mature form was lower than that of wild-type CFTR. Previously, we have shown that the ability of Cys-less to produce Band C protein in BHK cells is dependent on (i) the growth of the cells at a reduced temperature of 27 °C and (ii)

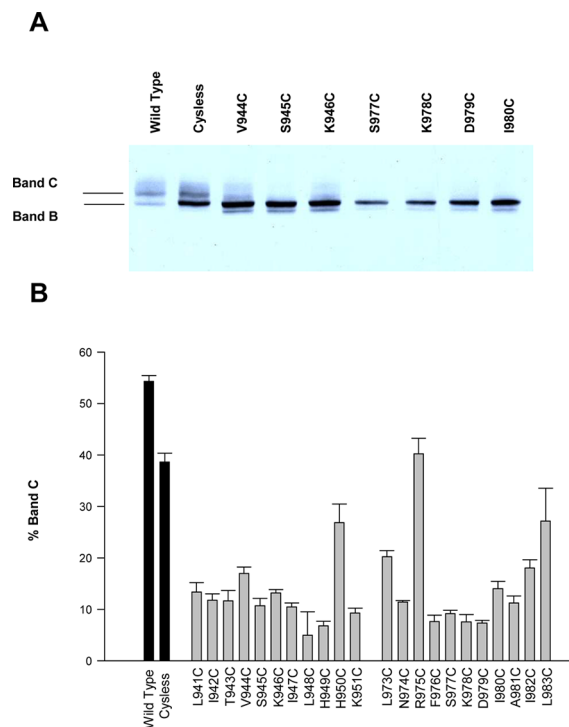


**Figure 2.** Protein expression of CL3 mutants. (A) Representative Western blot for CFTR using protein from BHK cells transfected with the wild type, the Cys-less mutant, or the named cysteine mutants in a Cys-less background. Note the near absence of Band C protein for these mutants. (B) Mean abundance of Band C protein (as a percentage of total). Only R975C was not significantly different from the Cys-less mutant ( $p > 0.6$ ); for H950C and L983C,  $p < 0.05$ , and for all other mutants,  $p < 0.00005$ . Means of data from nine independent transfections for Cys-less and three to six for other constructs are shown.

the presence of the V510A “rescue” mutation.<sup>32</sup> In contrast to the Cys-less background, almost all CL3 cysteine mutants studied gave almost undetectable levels of Band C protein (Figure 2), suggesting that mutations in this juxtamembrane region result in serious misprocessing of the CFTR protein.

**Effects of the MTS Reagents on Macroscopic Currents.** Functional properties of mutant CFTR expressed in BHK cells were investigated using inside-out patch recording. Sixteen of the 22 mutants that were constructed generated macroscopic PKA- and ATP-dependent currents in inside-out membrane patches (e.g., Figure 3). However, for the six remaining mutants (S945C, L948C, H949C, K951C, K978C, and D979C), application of PKA and ATP consistently failed to generate a significant increase in the macroscopic current amplitude above background levels. Each of these six mutants was also associated with undetectable levels of mature, Band C protein (Figure 2), suggesting that these mutants were misprocessed and absent from the cell membrane. However, other CL3 mutants with similar apparent misprocessing as determined by Western blotting (Figure 2) did generate measurable macroscopic currents. Our favored interpretation of this apparent discrepancy is that our patch clamp experiments are, in fact, able to detect tiny amounts of CFTR protein in the cell membrane that cannot be detected by Western blotting, either because the amount of mature Band C protein is below detection levels or because some immature Band B protein is present at the membrane. However, on the basis of our results,

we cannot rule out the alternative explanation that S945C, L948C, H949C, K951C, K978C, and D979C are also present at the cell membrane but that these mutants generate CFTR channels that are functionally nonresponsive to PKA and ATP.

For those 16 CL3 mutants that could be studied functionally, modification of introduced cysteines by negatively charged MTSES and positively charged MTSET was investigated by application of these reagents to the cytoplasmic face of inside-out membrane patches following channel activation by PKA and ATP. Three different types of functional effects were observed. In most cases (L941C, I942C, K946C, I947C, H950C, L973C, N974C, S977C, I980C, A981C, and I982C), macroscopic currents were inhibited by both MTSES and MTSET (e.g., Figure 3A). In contrast, T943C, V944C, and R975C were inhibited by MTSES but not significantly affected by MTSET exposure (e.g., Figure 3B). Two mutants, F976C and L983C, were not significantly affected by either MTSES or MTSET (e.g., Figure 3C), as recently demonstrated for Cys-less using similar protocols<sup>28,30</sup> (Figure 4). The shape of the macroscopic  $I$ - $V$  relationship was nearly linear for Cys-less CFTR<sup>28</sup> and was not significantly altered by any of the mutations studied, nor did modification by either MTSES or MTSET have any significant effect on the shape of the  $I$ - $V$  relationship (Figure 3D,E and Figure S1 of the Supporting Information). The effects of MTS reagents on the amplitude of macroscopic currents carried by different channel constructs are summarized in Figure 4. The rate of modification of introduced cysteines was quantified from the time course of macroscopic current amplitude change following application of MTSES or MTSET (Figure 5).

**Effects of MTSES on Single-Channel Currents.** To further characterize the nature of the inhibitory effects of MTS reagents on cysteine-substituted CL3 mutants, we recorded single-channel currents carried by these mutants in inside-out patches. For technical reasons, single-channel recordings were taken using a low extracellular  $\text{Cl}^-$  concentration of 4 mM (see Materials and Methods). Under these conditions, all channel constructs studied had identical single-channel conductance, even where the mutation involved removal of a positive charge (K946C and R975C) (Figure 6). Note that those six mutants that failed to generate macroscopic currents (see above) were also not associated with detectable single-channel currents.

We restricted our single-channel studies to the use of MTSES, because this reagent had more consistent effects on cysteine-substituted CL3 mutants [i.e., all MTS-sensitive mutants were inhibited by MTSES, although not all were inhibited by MTSET (Figure 4)] and also because we considered modification by this negatively charged substance more likely to interfere electrostatically with  $\text{Cl}^-$  permeation and so more likely to influence  $\text{Cl}^-$  conductance.<sup>28–30</sup> In fact, in most cases, MTSES and MTSET had similar effects on macroscopic current amplitudes (Figure 4). The approach we followed is illustrated in Figure 7, using I982C as an example. PKA- and ATP-stimulated single-channel currents were recorded for >5 min to ensure stable activation, following which MTSES was applied to the intracellular solution. In the example shown in Figure 7, it can be seen that the application of MTSES reduced the open probability of the channel to ~55% of the control, without affecting the single-channel current amplitude. Effects of MTSES on both unitary current amplitude and open probability were quantified using all-points amplitude histograms constructed from data before and after MTSES exposure (e.g., Figure 7B). This data for all channel

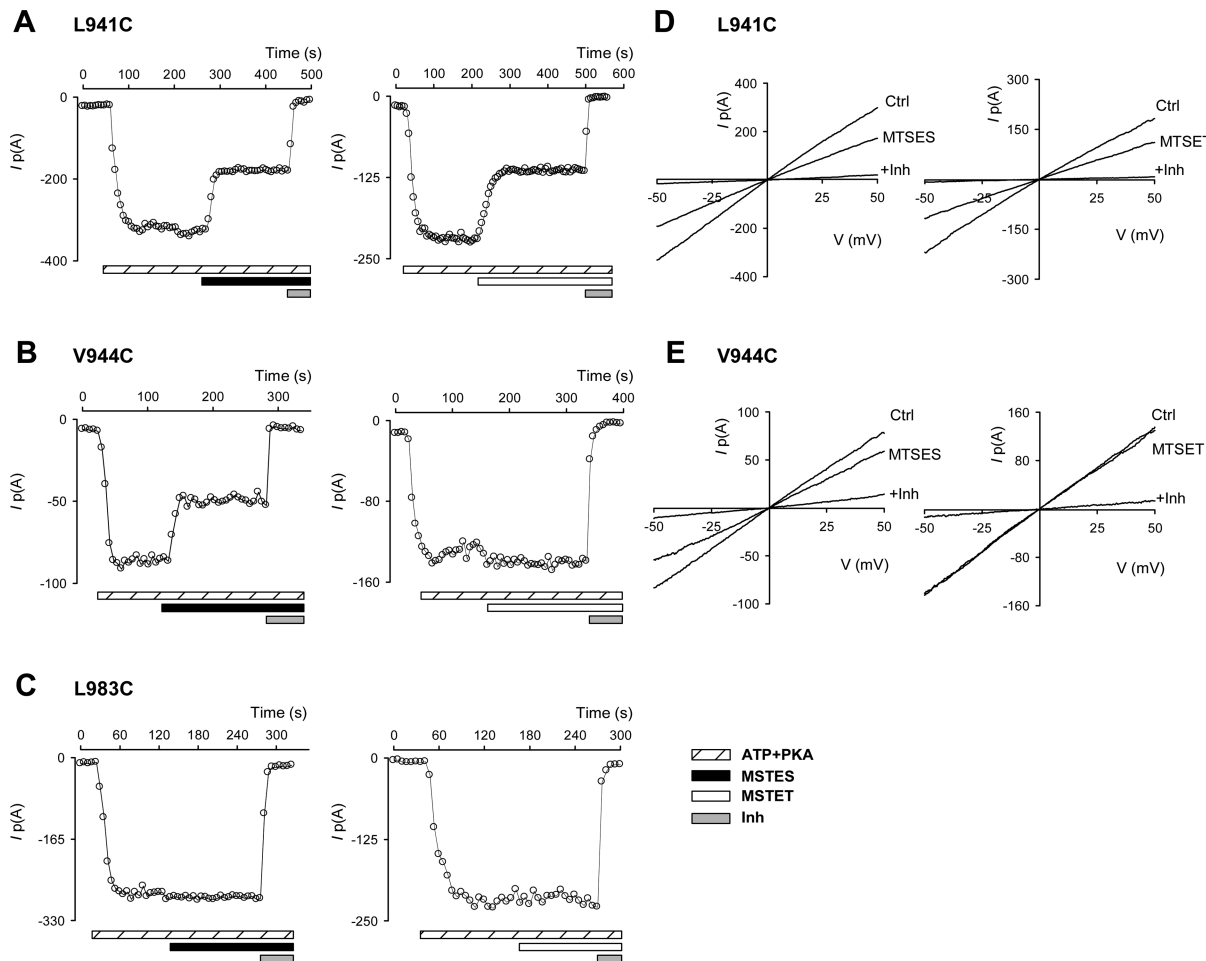


**Figure 3.** Modification of cysteines introduced into CL3 by internal MTS reagents. (A–C) Example time courses of macroscopic currents (measured at  $-50$  mV) carried by L941C (A), V944C (B), and L983C (C). After patch excision and recording of baseline currents, patches were treated sequentially with 20 nM PKA and 1 mM ATP (hatched bars), 200  $\mu$ M MTS reagent (left panels, MTSES, black bars; right panels, MTSET, white bars), and 5  $\mu$ M CFTR<sub>inh</sub>-172 (gray bars). (D and E)  $I$ – $V$  relationships for the patches shown in panels A and B following maximal current stimulation with PKA and ATP (control), following addition of MTSES (left panels) or MTSET (right panels), and following addition of CFTR<sub>inh</sub>-172 (+Inh).

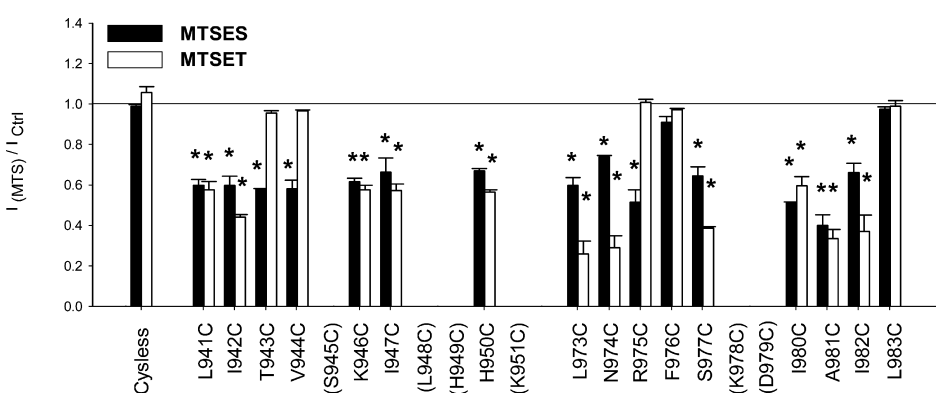


**Figure 4.** Effects of internal MTS reagents on macroscopic current amplitudes. Mean effect of treatment with 200  $\mu$ M MTSES (black bars) or MTSET (white bars) on the macroscopic current amplitude measured at  $-50$  mV, for Cys-less CFTR and each of the cysteine-substituted CL3 mutants named. Mutants that did not yield measurable macroscopic currents in inside-out patches are shown in parentheses. Means of data from three or four patches are shown. Asterisks indicate a significant difference from the value of Cys-less ( $p < 0.05$ ).

constructs studied are summarized in Figure 8. In no case did MTSES exposure significantly affect single-channel current amplitude (Figure 8A). In contrast, for all mutants for which MTSES exposure reduced macroscopic current amplitudes (Figure 4), MTSES also caused a reduction in open probability

(Figure 8B). MTSES did not affect open probability in Cys-less, or in two mutants that were not sensitive to MTSES at the macroscopic current level [F976C and L983C (Figure 4)] (Figure 8B), suggesting that it is an MTSES-induced reduction in open probability that is responsible for the reduction in

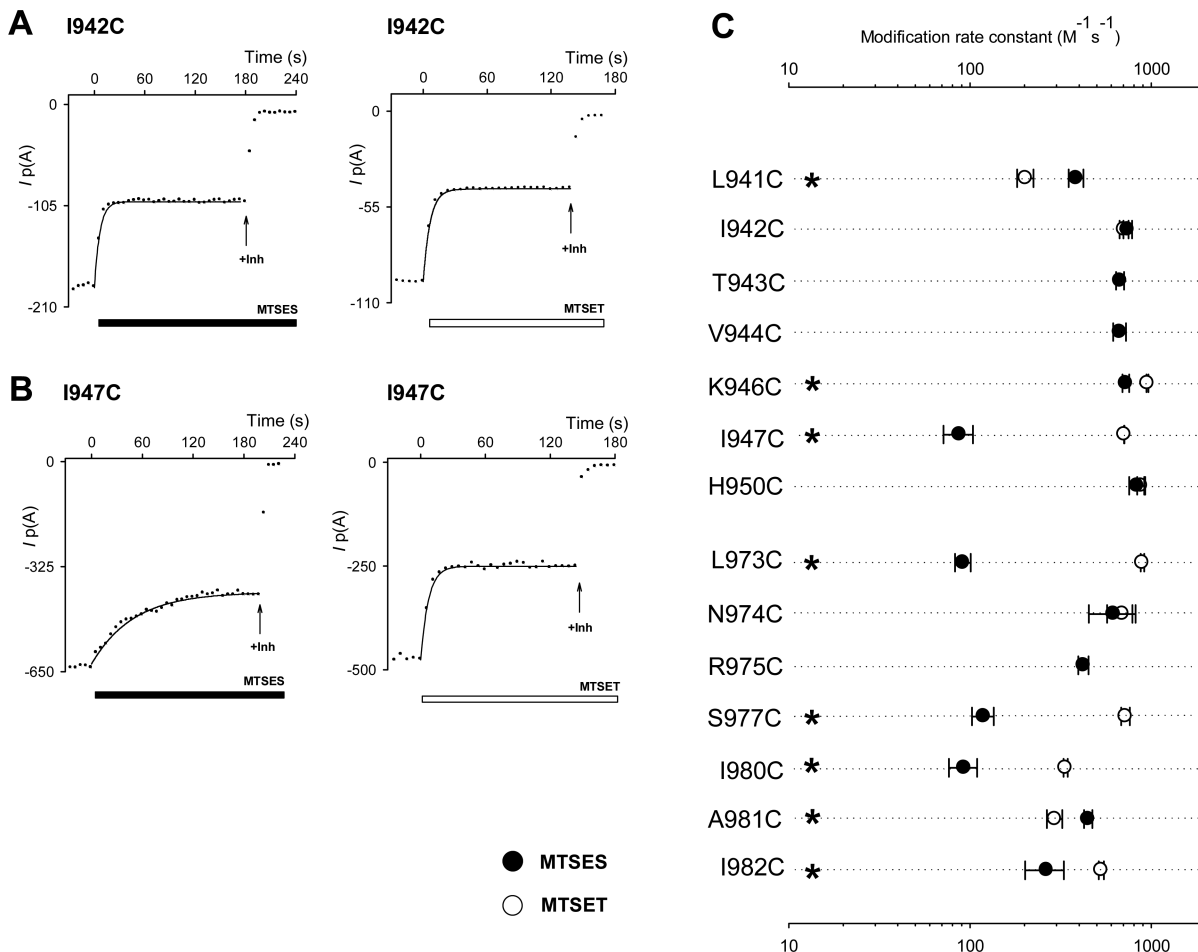


**Figure 5.** Rate of modification by MTSES and MTSET. (A and B) Example time courses of macroscopic currents (measured at  $-50$  mV) carried by I942C (A) and I947C (B). Current amplitudes were measured every 6 s after attainment of stable current amplitude following activation by PKA (20 nM) and ATP (1 mM). In each case, 200  $\mu$ M MTSES (black bars) or MTSET (white bars) was applied to the cytoplasmic face of the patch at time zero. The decline in current amplitude due to MTS modification has been fit by a single-exponential function in each case. Currents remaining in the presence of MTSES or MTSET were inhibited by application of 5  $\mu$ M CFTR<sub>inh</sub>-172 as indicated. (C) Calculated modification rate constants for both MTSES (●) and MTSET (○) for each of the 14 MTS reagent-sensitive mutants listed. Note that T943C, V944C, and R975C were inhibited by MTSES but not by MTSET (see Figure 4). Means of data from three patches are shown. Asterisks indicate a significant difference between the modification rate constant for MTSES and that for MTSET ( $p < 0.05$ ).

macroscopic current amplitude due to MTSES modification observed in Figure 4.

## DISCUSSION

Of 22 cysteine mutations introduced into CL3, 21 appeared to be associated with a significant defect in protein processing relative to the Cys-less background, as determined by densitometric analysis of production of mature CFTR protein (Figure 2). Superficially, this might appear to support an important, and relatively non-site-specific, role for CL3 in normal CFTR processing (see the introductory section). However, Cys-less CFTR itself has a severe protein misprocessing defect<sup>32,34,35</sup> that in this study has been partially ameliorated by a rescue mutation in NBD1 (V510A) and by growing transfected BHK cells at a reduced temperature of 27 °C (see Materials and Methods). Thus, the relevance of these findings for the processing of wild-type CFTR is uncertain, as is the rationale for studying trafficking in a Cys-less CFTR background.

Interestingly, many CL3 mutants could be studied functionally in spite of an apparent lack of mature protein (Figure 2).

We believe this most likely reflects the sensitivity of our patch clamp assay to the presence of even very small amounts of CFTR in the cell membrane. Only six mutants (S945C, L948C, H949C, K951C, K978C, and D979C) failed to generate functional channels in inside-out membrane patches (Figure 4). Each of these six was associated with undetectable Band C protein by Western blotting (Figure 2), consistent with the failure of trafficking of these mutants to the cell membrane. Misprocessing of CF-associated mutants S945L, H949Y, and D979A has previously been demonstrated,<sup>17,20</sup> perhaps indicating that these residues are particularly critical for normal protein processing. However, because our work failed to show a direct correlation between protein processing determined biochemically (Figure 2) and function determined electrophysiologically (Figure 4), we cannot rule out the possibility that the six nonfunctional mutants are present in the cell membrane but nonfunctional for other reasons, such as a failure to open in response to ATP and PKA or an undetectably low single-channel conductance.

Interestingly, one mutant that failed to express functional channels in our hands (K978C) has previously been studied in a Cys-less background by patch clamp recording by others<sup>18</sup>

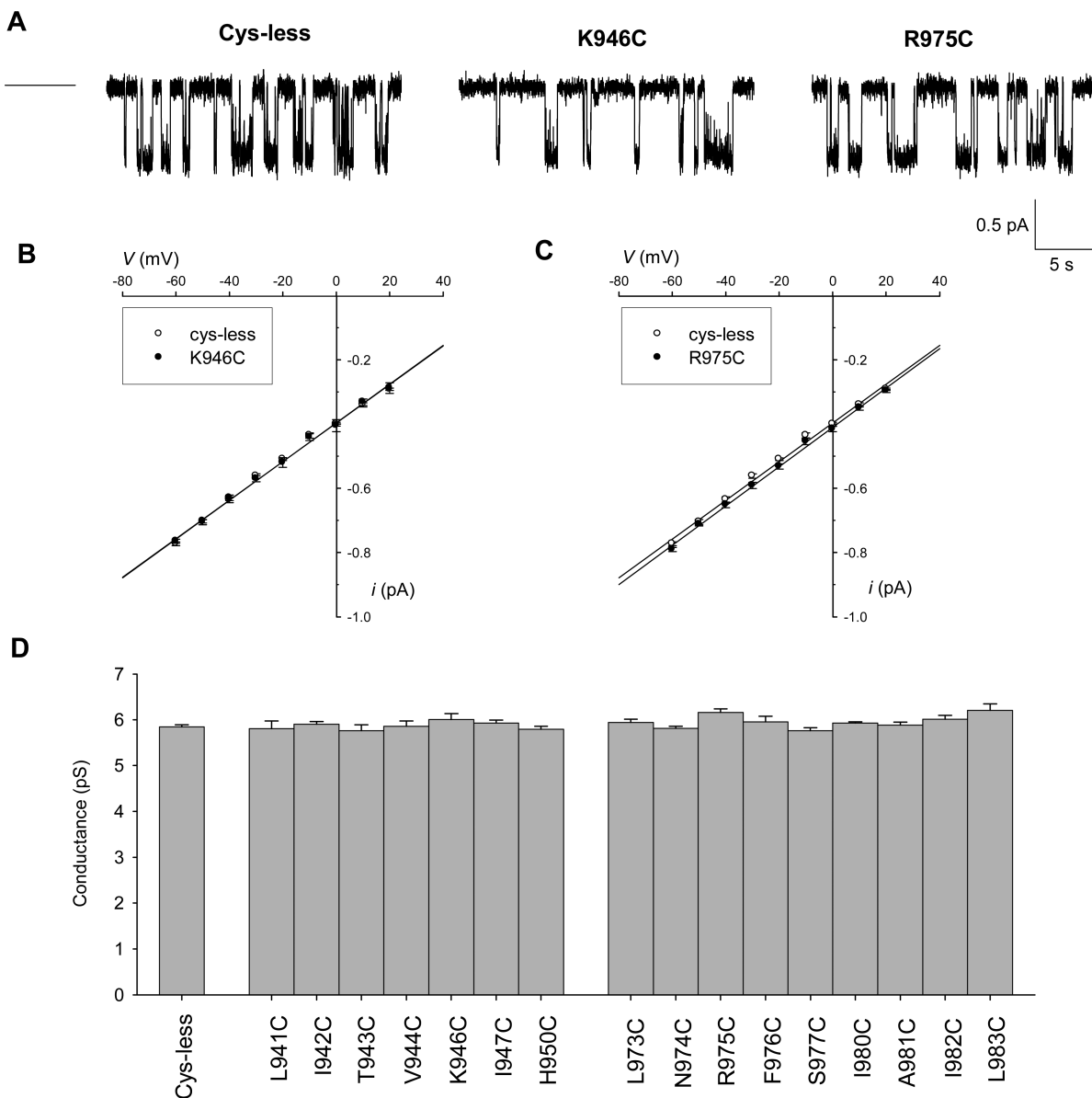


**Figure 6.** Single-channel conductance of cysteine mutants. (A) Example single-channel currents carried by Cys-less CFTR and the charge-substituting mutants K946C and R975C as indicated, at a membrane potential of  $-50$  mV. The horizontal line to the left of the traces indicates the channel closed state current level. (B and C) Mean single-channel  $I$ – $V$  relationships recorded under these conditions for Cys-less (○), K946C (●, B), and R975C (●, C). (D) Mean single-channel conductance for different channel variants measured under these conditions. None of these were significantly different from the Cys-less background. Means of data from three to twelve patches are shown in panels C and D.

(see below). Results with this mutant, which was shown to generate constitutively active (ATP-independent) channel, formed a central part of the hypothesis put forward by Wang et al.<sup>18</sup> concerning the role of CL3 in channel gating. It was a great surprise to us, therefore, that we were unable to observe functional expression of K978C in our experiments (Figure 3), especially as Wang et al.<sup>18</sup> had also studied this mutant in a Cys-less background. Because we were so surprised at not being able to replicate the functional expression of this mutant, we in fact constructed this mutant on three independent occasions, but in each case, the lack of functional expression remained the same. We can only imagine that some difference in the expression system has resulted in our failure to observe currents for this mutant. Indeed, our results indicate that this mutant is associated with a severe protein processing defect in BHK cells (Figure 2). In fact, the functional results of Wang et al.<sup>18</sup> for

K978C, that the open probability of the channel is reduced following modification by MTSET, are quite consistent with our own findings for other, nearby CL3 residues.

Our focus in this work was to explore the functional properties of CL3 mutants that do express functional channels in the membrane of BHK cells. We found that 14 of 16 functional cysteine-substituted mutants were sensitive to cytoplasmic exposure to MTSES and/or MTSET (Figure 4). This suggests that most of the juxtamembrane parts of CL3 (Figure 1) are exposed to the cytoplasm and readily accessible to large cytoplasmic substances. In fact, there was no apparent difference between those mutations located proximal to TM8 compared to those proximal to TM9, in terms of the functional effect of modification (Figure 4) or the rate of modification (Figure 5), suggesting that these two “limbs” of CL3 show approximately equivalent accessibilities to the cytoplasm. We

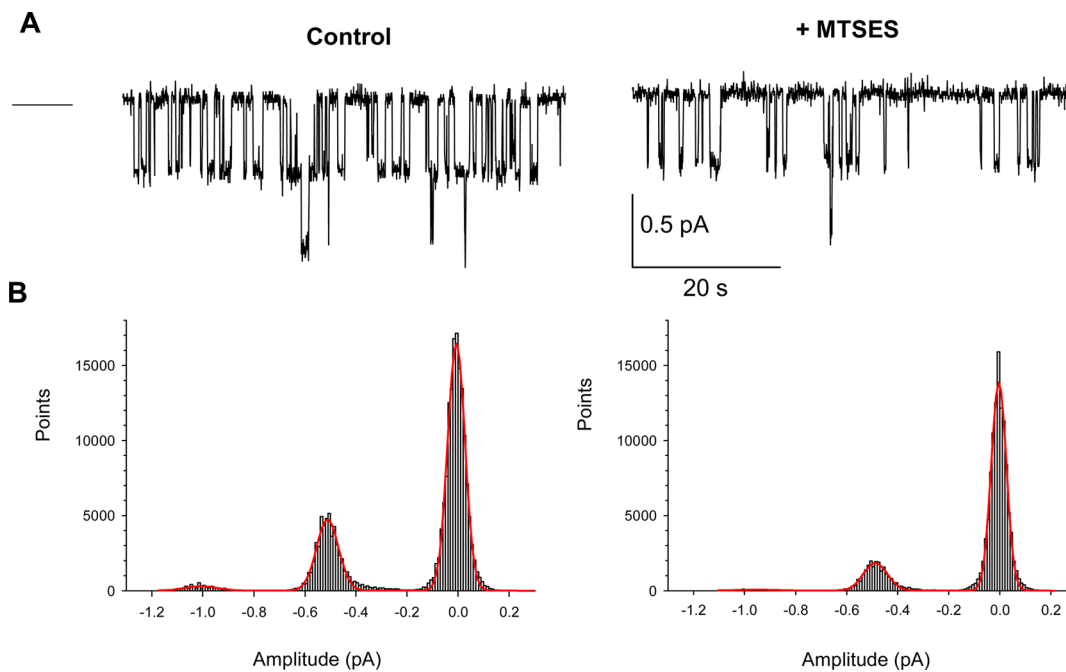


**Figure 7.** Example of the effect of modification by MTSES on single-channel currents. (A) Current recorded from a patch containing two I982C channels, before (Control) and after addition of 200  $\mu\text{M}$  MTSES to the intracellular solution, at a membrane potential of -20 mV. The horizontal line to the left of the traces indicates the zero current level. (B) All-points amplitude histograms prepared from extended periods of the recordings shown in panel A, corresponding to control (left) and post-MTSES (right) conditions. Each has been fit by the sum of three Gaussian functions, giving mean unitary amplitudes of -0.504 pA (control) and -0.488 pA (+MTSES) and open probabilities of 0.183 (control) and 0.101 (+MTSES).

reasoned that the reduction in macroscopic current amplitude that consistently resulted from MTSES and/or MTSET modification of CL3 (Figure 4) could reflect a reduction in  $\text{Cl}^-$  conductance (i.e., interference with the movement of  $\text{Cl}^-$  through the open channel pore) and/or a reduction in open probability (i.e., interference with the normal opening and closing of the channel). Direct single-channel recording experiments with MTSES (Figures 7 and 8) support the latter explanation. However, we have additional reasons to doubt an important functional role for CL3 in influencing the functional properties of the permeation pathway for  $\text{Cl}^-$  ions.

We<sup>2,28,30</sup> and others<sup>3,29</sup> have recently used cytoplasmic MTS reagents to identify pore-lining amino acid side chains in TM1, TM6, and TM12, and several patterns emerge from these studies. In each of these studies, MTSES modification inside the pore always causes a reduction in channel function, most likely because of interference with  $\text{Cl}^-$  permeation. This contrasts with MTSES modification of CL3, which has no effect on  $\text{Cl}^-$  conductance (Figure 8A). It would be most surprising if introduction of a negative charge by covalent modification by MTSES close to the permeation pathway for  $\text{Cl}^-$  ions did not alter  $\text{Cl}^-$  conductance. The rate of MTSES modification is high for cysteines introduced close to the cytoplasmic ends of the TMs and decreases with the apparent distance into the pore from its cytoplasmic end, consistent with narrowing of the pore.<sup>2,28,30</sup> In contrast, there was no apparent pattern to the rate of MTS modification of different CL3 residues (Figure 5). Importantly, in TM1 the rate of modification by positively charged MTSET is consistently ~10-fold lower than that by negatively charged MTSES, which was interpreted as reflecting the function of the CFTR channel as an anion-selective pore.<sup>30</sup> In contrast, although some differences in the rate of MTSES versus MTSET modification were observed for some CL3 residues (Figure 5), there was no consistent pattern suggestive

of an overall anion selectivity of this region of CFTR. Instead, we suggest that local factors may result in the small differences in the rate of MTSES versus MTSET modification measured at specific CL3 residues (Figure 5). The effects of cysteine substitutions per se also do not support an important role for the juxtamembrane regions of CL3 in the  $\text{Cl}^-$  permeation pathway. None of the mutants studied altered the shape of the macroscopic  $I-V$  curve (Figure S1 of the Supporting Information) or the single-channel conductance (Figure 6), even though both of these parameters are highly sensitive to cysteine substitutions both in the TMs<sup>28,29,33,39–42</sup> and in the ELs that are thought to contribute to the outer mouth of the pore.<sup>4,5</sup> The shapes of the  $I-V$  relationships were also not altered by MTSES or MTSET modification (Figure S1 of the Supporting Information), even though the charge deposition associated with MTS modification often affects the rectification of the  $I-V$  relationship for cysteines located close to the  $\text{Cl}^-$  permeation pathway.<sup>4,5,28,33,41,42</sup>

Overall, our findings suggest that, even though molecular models of CFTR suggest that the juxtamembrane region of CL3 might contribute to a restricted region of a central "pore" through the MSDs (Figure 1), this region does not make a sufficiently important functional contribution to the channel to significantly influence  $\text{Cl}^-$  permeation. One possibility is that CL3 does line the aqueous lumen of the pore, but that  $\text{Cl}^-$  ions do not approach close enough to CL3 for their movement to be influenced by the properties of individual amino acid side chains here. This would imply that the open pore is very wide at the level of the CLs, much wider than in the TMs where  $\text{Cl}^-$  ions certainly do interact with pore-lining side chains. This suggestion would be consistent with longstanding functional data suggesting the pore has a deep and wide inner vestibule that is readily accessible to large cytoplasmic substances in open channels.<sup>1,43</sup> However, it is in direct contrast with the idea,

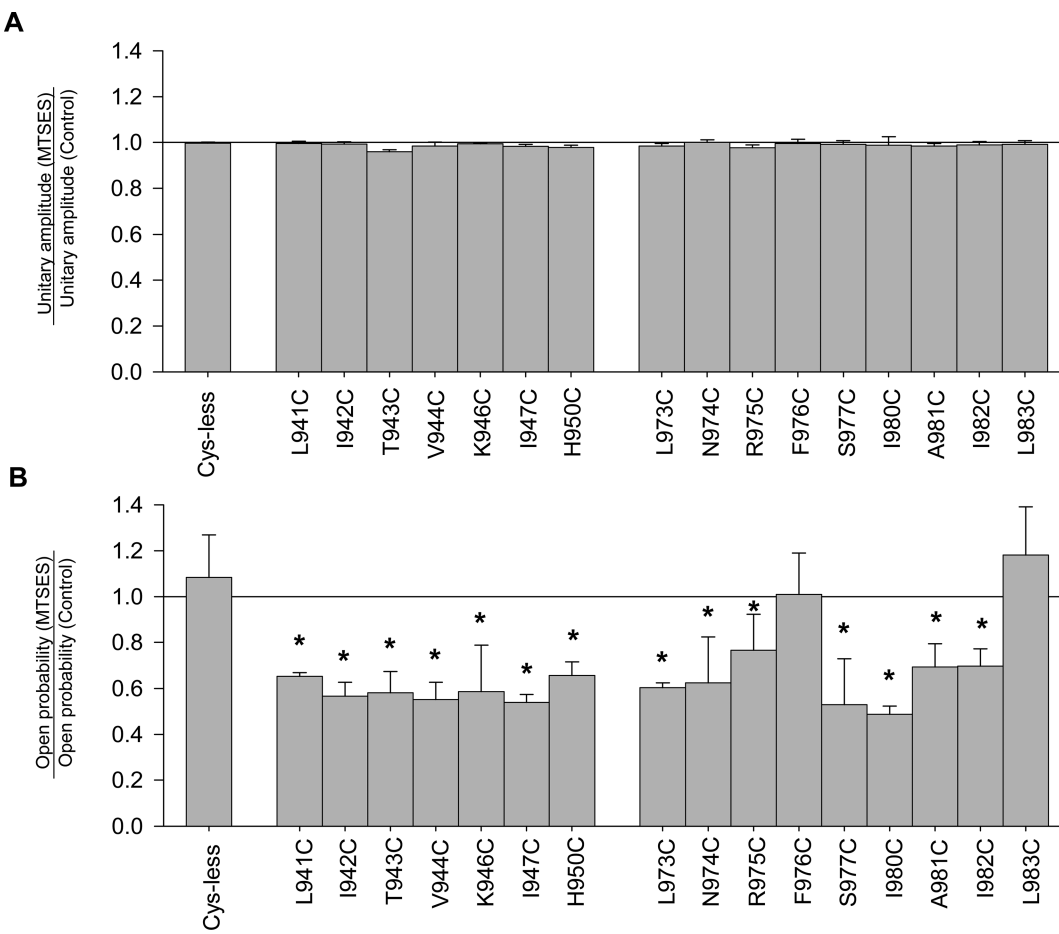


**Figure 8.** Effects of MTSES on the single-channel current amplitude and open probability. Single-channel recordings such as those shown in Figure 7 were used to quantify the effect of MTSES (200  $\mu$ M) on the single-channel current amplitude (A) and open probability (B) for each of the channel variants named. Means of data from three to nine patches are shown. Asterisks indicate a significant difference from Cys-less ( $p < 0.05$ ).

based on homology modeling, that the CLs form a physically narrow region of the pore (Figure 1).<sup>11</sup> It is also possible that other CLs make a more important functional contribution than CL3 does, although the model shown in Figure 1 suggests a fairly symmetrical contribution of all four CLs to the apparent central pore. An alternative possibility is that this central pore apparently formed by the CLs (Figure 1C) is not part of the Cl<sup>-</sup> permeation pathway at all. In some ion channel types, the permeant ion does not follow a direct pathway along the central axis of the entire protein but instead enters and exits a central transmembrane pore via lateral “portals” located close to the cytoplasmic side of the membrane.<sup>44–48</sup> There is no functional evidence of the existence of such portals in CFTR, although we would point out that there is also no direct evidence that Cl<sup>-</sup> ions enter the permeation pathway at the cytoplasmic end of the CLs and pass along the extent of the central axis of the channel protein. Interestingly, a recent direct structural study of CFTR suggested that portals might exist at the TM5–CL2 and TM11–CL4 cytoplasmic boundaries.<sup>49</sup> In many ABC proteins, the substrate translocation pathway is partially open to part of the lipid bilayer, raising the possibility that some substrates enter and exit via the bilayer.<sup>50</sup> As described by Bai et al.,<sup>29</sup> such an opening to the bilayer, which can actually be observed at the extracellular end of the CFTR structural model of Figure 1A, is inconsistent with the function of CFTR as an ion channel. Nevertheless, these openings do raise the precedent that ABC

protein substrates do not necessarily follow an unwaveringly central path through the protein.

Our results do support the previously suggested role for CL3 in gating of the CFTR channel.<sup>14–18</sup> MTSES modification of 14 of 16 functional cysteine-substituted mutants led to a decrease in channel open probability (Figure 8B), even though the mutations themselves did not appear to have dramatic effects on open probability (Figure S2 of the Supporting Information). In most cases, MTSET had a similar effect (Figure 4), indicating a lack of strong charge dependence in the functional effects of modification. The consistent effects of MTS modification (Figure 4) argue against a specific role for individual amino acid side chains in CL3 in channel gating and instead suggest that changes in the structure of this CL exert a relatively nonspecific effect on gating. This would appear to be consistent with the hypothesis put forward by Wang et al.<sup>18</sup> that CL3 forms a “compression spring” that regulates the opening and closing of the channel. Modification by MTS reagents may then stiffen the spring and reduce the open probability in a relatively position-independent fashion. This hypothesis emphasizes the role of the CLs in transmitting gating information “forward” from the NBDs to the pore. It is also possible that the CLs are involved in transmitting gating information “backward”, i.e., that changes in the structure of CL3 feed back to modify NBD function, ultimately resulting in a change in channel gating.<sup>29,51</sup> Irrespective of the precise mechanism, our similar results for mutations in the two limbs of

CL3 suggest these regions of the protein play similar functional roles. Furthermore, because MTS modification of most residues resulted in a similar, ~25–75% inhibition of the macroscopic current amplitude, it might be considered that no sites in CL3 are absolutely essential to channel function, perhaps pointing to a role of this region as a mediator, rather than a controller, of channel gating.

In summary, our comprehensive functional screening of CL3 suggests that this region of CFTR is readily accessible to the cytoplasm, where it plays a role in the control of channel gating. This is consistent with the prevailing idea that CL3 forms the link between the site of ATP action (the NBDs) and the opening and closing of a channel gate located in the TMs. However, our results do not support the hypothesis that this region is close enough to the Cl<sup>-</sup> permeation pathway to exert any influence on permeating Cl<sup>-</sup> ions.

## ■ ASSOCIATED CONTENT

### Supporting Information

Two figures as described in the text. This material is available free of charge via the Internet at <http://pubs.acs.org>.

## ■ AUTHOR INFORMATION

### Corresponding Author

\*Phone: (902) 494-2265. Fax: (902) 494-1685. E-mail: paul.linsdell@dal.ca.

### Funding

This work was supported by the Canadian Institutes of Health Research. Y.E.H. is a Cystic Fibrosis Canada Postdoctoral Fellow.

### Notes

The authors declare no competing financial interest.

## ■ ABBREVIATIONS

ABC, ATP-binding cassette; BHK, baby hamster kidney; CFTR, cystic fibrosis transmembrane conductance regulator; CL, cytoplasmic loop; EL, extracellular loop; MSD, membrane-spanning domain; MTS, methanethiosulfonate; MTSES, [2-sulfonatoethyl] methanethiosulfonate; MTSET, [2-(trimethylammonium)ethyl] methanethiosulfonate; NBD, nucleotide binding domain; PKA, protein kinase A; SCAM, substituted cysteine accessibility mutagenesis; TM, transmembrane  $\alpha$ -helix.

## ■ REFERENCES

- Linsdell, P. (2006) Mechanism of chloride permeation in the cystic fibrosis transmembrane conductance regulator chloride channel. *Exp. Physiol.* 91, 123–129.
- Qian, F., El Hiani, Y., and Linsdell, P. (2011) Functional arrangement of the 12th transmembrane region in the CFTR chloride channel pore based on functional investigation of a cysteine-less CFTR variant. *Pfluegers Arch.* 462, 559–571.
- Bai, Y., Li, M., and Hwang, T.-C. (2011) Structural basis for the channel function of a degraded ABC transporter, CFTR (ABCC7). *J. Gen. Physiol.* 138, 495–507.
- Zhou, J.-J., Fatehi, M., and Linsdell, P. (2008) Identification of positive charges situated at the outer mouth of the CFTR chloride channel pore. *Pfluegers Arch.* 457, 351–360.
- Fatehi, M., and Linsdell, P. (2009) Novel residues lining the CFTR chloride channel pore identified by functional modification of introduced cysteines. *J. Membr. Biol.* 228, 151–164.
- Hwang, T.-C., and Sheppard, D. N. (2009) Gating of the CFTR Cl<sup>-</sup> channel by ATP-driven nucleotide-binding domain dimerisation. *J. Physiol.* 587, 2151–2161.
- Muallem, D., and Vergani, P. (2009) ATP hydrolysis-driven gating in cystic fibrosis transmembrane conductance regulator. *Philos. Trans. R. Soc. London, Ser. B* 364, 247–255.
- Wang, W., and Linsdell, P. (2012) Conformational change opening the CFTR chloride channel pore coupled to ATP-dependent gating. *Biochim. Biophys. Acta* 1818, 851–860.
- Mornon, J.-P., Lehn, P., and Callebaut, I. (2008) Atomic model of human cystic fibrosis transmembrane conductance regulator: Membrane-spanning domains and coupling interfaces. *Cell. Mol. Life Sci.* 65, 2594–2612.
- Serohijos, A. W. R., Hegedüs, T., Aleksandrov, A. A., He, L., Cui, L., Dokholyan, N. V., and Riordan, J. R. (2008) Phenylalanine-508 mediates a cytoplasmic-membrane domain contact in the CFTR 3D crystal structure crucial to assembly and channel function. *Proc. Natl. Acad. Sci. U.S.A.* 105, 3256–3261.
- Mornon, J.-P., Lehn, P., and Callebaut, I. (2009) Molecular models of the open and closed states of the whole human CFTR protein. *Cell. Mol. Life Sci.* 66, 3469–3486.
- Locher, K. P. (2009) Structure and mechanism of ATP-binding cassette transporters. *Philos. Trans. R. Soc. London, Ser. B* 364, 239–245.
- Kerr, I. D., Jones, P. M., and George, A. M. (2010) Multidrug efflux pumps: The structure of prokaryotic ATP-binding cassette transporter efflux pumps and implications for our understanding of eukaryotic P-glycoproteins and homologues. *FEBS J.* 277, 550–563.
- He, L., Aleksandrov, A. A., Serohijos, A. W. R., Hegedüs, T., Aleksandrov, L. A., Cui, L., Dokholyan, N. V., and Riordan, J. R. (2008) Multiple membrane-cytoplasmic domain contacts in the cystic fibrosis transmembrane conductance regulator (CFTR) mediate regulation of channel gating. *J. Biol. Chem.* 283, 26383–26390.
- Wang, G. (2010) State-dependent regulation of cystic fibrosis transmembrane conductance regulator (CFTR) gating by a high affinity Fe<sup>3+</sup> bridge between the regulatory domain and cytoplasmic loop 3. *J. Biol. Chem.* 285, 40438–40447.
- Wang, G. (2011) The inhibition mechanism of non-phosphorylated Ser<sup>768</sup> in the regulatory domain of cystic fibrosis transmembrane conductance regulator. *J. Biol. Chem.* 286, 2171–2182.
- Seibert, F. S., Linsdell, P., Loo, T. W., Hanrahan, J. W., Riordan, J. R., and Clarke, D. M. (1996) Cytoplasmic loop three of cystic fibrosis transmembrane conductance regulator contributes to regulation of chloride channel activity. *J. Biol. Chem.* 271, 27493–27499.
- Wang, W., Wu, J., Bernard, K., Li, G., Wang, G., Bevensee, M. O., and Kirk, K. L. (2010) ATP-independent CFTR channel gating and allosteric modulation by phosphorylation. *Proc. Natl. Acad. Sci. U.S.A.* 107, 3888–3893.
- Kirk, K. L., and Wang, W. (2011) A unified view of cystic fibrosis transmembrane conductance regulator (CFTR) gating: Combining the allosterism of a ligand-gated channel with the enzymatic activity of an ATP-binding cassette (ABC) transporter. *J. Biol. Chem.* 286, 12813–12819.
- Clain, J., Fritsch, J., Lehmann-Che, J., Bali, M., Arous, N., Goossens, M., Edelman, A., and Fanen, P. (2001) Two mild cystic fibrosis-associated mutations result in severe cystic fibrosis when combined in cis and reveal a residue important for cystic fibrosis transmembrane conductance regulator processing and function. *J. Biol. Chem.* 276, 9045–9049.
- Cui, L., Aleksandrov, L., Chang, X.-B., Hou, Y.-X., He, L., Hegedüs, T., Gentzsch, M., Aleksandrov, A., Balch, W. E., and Riordan, J. R. (2007) Domain interdependence in the biosynthetic assembly of CFTR. *J. Mol. Biol.* 365, 981–994.
- Loo, T. W., Bartlett, M. C., and Clarke, D. M. (2008) Processing mutations disrupt interactions between the nucleotide binding and transmembrane domains of P-glycoprotein and the cystic fibrosis transmembrane conductance regulator (CFTR). *J. Biol. Chem.* 283, 28190–28197.
- Lukacs, G. L., and Verkman, A. S. (2012) CFTR: Folding, misfolding and correcting the ΔF508 conformational defect. *J. Mol. Med.* 18, 81–91.

- (24) Drévillon, L., Tanguy, G., Hinzpeter, A., Arous, N., de Bechedière, A., Aissat, A., Tarze, A., Goossens, M., and Fanen, P. (2011) COMMD1-mediated ubiquitination regulates CFTR trafficking. *PLoS One* 6, e18334.
- (25) Melin, P., Hosy, E., Vivaudou, M., and Becq, F. (2007) CFTR inhibition by glibenclamide requires a positive charge in cytoplasmic loop three. *Biochim. Biophys. Acta* 1768, 2438–2446.
- (26) Li, M.-S., Holstead, R. G., Wang, W., and Linsdell, P. (2011) Regulation of CFTR chloride channel macroscopic conductance by extracellular bicarbonate. *Am. J. Physiol.* 300, C65–C74.
- (27) Alexander, C., Ivetac, A., Liu, X., Norimatsu, Y., Serrano, J. R., Landstrom, A., Sansom, M., and Dawson, D. C. (2009) Cystic fibrosis transmembrane conductance regulator: Using differential reactivity toward channel-permeant and channel-impermeant thiol-reactive probes to test a molecular model for the pore. *Biochemistry* 48, 10078–10088.
- (28) El Hiani, Y., and Linsdell, P. (2010) Changes in accessibility of cytoplasmic substances to the pore associated with activation of the cystic fibrosis transmembrane conductance regulator chloride channel. *J. Biol. Chem.* 285, 32126–32140.
- (29) Bai, Y., Li, M., and Hwang, T.-C. (2010) Dual roles of the sixth transmembrane segment of the CFTR chloride channel in gating and permeation. *J. Gen. Physiol.* 136, 293–309.
- (30) Wang, W., El Hiani, Y., and Linsdell, P. (2011) Alignment of transmembrane regions in the cystic fibrosis transmembrane conductance regulator chloride channel pore. *J. Gen. Physiol.* 138, 165–178.
- (31) Mense, M., Vergani, P., White, D. M., Altberg, G., Nairn, A. C., and Gadsby, D. C. (2006) *In vivo* phosphorylation of CFTR promotes formation of a nucleotide-binding domain heterodimer. *EMBO J.* 25, 4728–4739.
- (32) Li, M.-S., Demsey, A. F. A., Qi, J., and Linsdell, P. (2009) Cysteine-independent inhibition of the CFTR chloride channel by the cysteine-reactive reagent sodium (2-sulphonatoethyl) methanethio-sulphonate (MTSES). *Br. J. Pharmacol.* 157, 1065–1071.
- (33) St. Aubin, C. N., and Linsdell, P. (2006) Positive charges at the intracellular mouth of the pore regulate anion conduction in the CFTR chloride channel. *J. Gen. Physiol.* 128, 535–545.
- (34) Loo, T. W., and Clarke, D. M. (2006) Using a cysteine-less mutant to provide insight into the structure and mechanism of CFTR. *J. Physiol.* 572, 312.
- (35) Wang, Y., Loo, T. W., Bartlett, M. C., and Clarke, D. M. (2007) Correctors promote maturation of cystic fibrosis transmembrane conductance regulator (CFTR)-processing mutants by binding to the protein. *J. Biol. Chem.* 282, 33247–33251.
- (36) Cui, L., Aleksandrov, L., Hou, Y.-X., Gentzsch, M., Chen, J.-H., Riordan, J. R., and Aleksandrov, A. A. (2006) The role of cystic fibrosis transmembrane conductance regulator phenylalanine 508 side chain in ion channel gating. *J. Physiol.* 572, 347–358.
- (37) Holstead, R. G., Li, M.-S., and Linsdell, P. (2011) Functional differences in pore properties between wild type and cysteine-less forms of the CFTR chloride channel pore. *J. Membr. Biol.* 243, 15–23.
- (38) Gong, X., Burbridge, S. M., Cowley, E. A., and Linsdell, P. (2002) Molecular determinants of  $\text{Au}(\text{CN})_2^-$  binding and permeability within the cystic fibrosis transmembrane conductance regulator  $\text{Cl}^-$  channel pore. *J. Physiol.* 540, 39–47.
- (39) Smith, S. S., Liu, X., Zhang, Z.-R., Sun, F., Kriewall, T. E., McCarty, N. A., and Dawson, D. C. (2001) CFTR: Covalent and noncovalent modification suggests a role for fixed charges in anion conduction. *J. Gen. Physiol.* 118, 407–431.
- (40) Zhang, Z.-R., Song, B., and McCarty, N. A. (2005) State-dependent chemical reactivity of an engineered cysteine reveals conformational changes in the outer vestibule of the cystic fibrosis transmembrane conductance regulator. *J. Biol. Chem.* 280, 41997–42003.
- (41) Fatehi, M., and Linsdell, P. (2008) State-dependent access of anions to the cystic fibrosis transmembrane conductance regulator chloride channel pore. *J. Biol. Chem.* 283, 6102–6109.
- (42) Zhou, J.-J., Li, M.-S., Qi, J., and Linsdell, P. (2010) Regulation of conductance by the number of fixed positive charges in the intracellular vestibule of the CFTR chloride channel pore. *J. Gen. Physiol.* 135, 229–245.
- (43) Hwang, T.-C., and Sheppard, D. N. (1999) Molecular pharmacology of the CFTR  $\text{Cl}^-$  channel. *Trends Pharmacol. Sci.* 20, 448–453.
- (44) Miyazawa, A., Fujiyoshi, Y., Stowell, M., and Unwin, N. (1999) Nicotinic acetylcholine receptor at 4.6 Å resolution: Transverse tunnels in the channel wall. *J. Mol. Biol.* 288, 765–786.
- (45) Gulbis, J. M., Zhou, M., Mann, S., and MacKinnon, R. (2000) Structure of the cytoplasmic  $\beta$  subunit: T1 assembly of voltage-dependent  $\text{K}^+$  channels. *Science* 289, 123–127.
- (46) Kelley, S. P., Dunlop, J. I., Kirkness, E. F., Lambert, J. J., and Peters, J. A. (2003) A cytoplasmic region determines single-channel conductance in 5-HT<sub>3</sub> receptors. *Nature* 424, 321–324.
- (47) Payandeh, J., Scheuer, T., Zheng, N., and Catterall, W. A. (2011) The crystal structure of a voltage-gated sodium channel. *Nature* 475, 353–358.
- (48) Samways, D. S., Khakh, B. S., Dutertre, S., and Egan, T. M. (2011) Preferential use of unobstructed lateral portals as the access route to the pore of human ATP-gated ion channels (P2X receptors). *Proc. Natl. Acad. Sci. U.S.A.* 108, 13800–13805.
- (49) Rosenberg, M. F., O’Ryan, L. P., Hughes, G., Zhao, Z., Aleksandrov, L. A., Riordan, J. R., and Ford, R. C. (2011) The cystic fibrosis transmembrane conductance regulator (CFTR): Three dimensional structure and localization of a channel gate. *J. Biol. Chem.* 286, 42647–42654.
- (50) Kos, V., and Ford, R. C. (2009) The ATP-binding cassette family: A structural perspective. *Cell. Mol. Life Sci.* 66, 3111–3126.
- (51) Kogan, I., Ramjeesingh, M., Huan, L.-J., Wang, Y., and Bear, C. E. (2001) Perturbation of the pore of the cystic fibrosis transmembrane conductance regulator (CFTR) inhibits its ATPase activity. *J. Biol. Chem.* 276, 11575–11581.